How to Cite:
Mohammed, M. K., & Wadday, F. Y. (2022). Synthesis, spectral properties and antibacterial studies of new hetrocyclic schiff-azo ligand derived from 5-amino 2-phenyl.4h-pyrazol-3-one with some transition metal complexes. *International Journal of Health Sciences*, *6*(S6), 11523–11542. https://doi.org/10.53730/ijhs.v6nS6.13199

Synthesis, spectral properties and antibacterial studies of new hetrocyclic schiff-azo ligand derived from 5-amino 2-phenyl.4h-pyrazol-3-one with some transition metal complexes

Muna Khallawi Mohammed
Ministry of Education, The General Directorate of Educational in Najaf Al-Ashraf, Najaf, Iraq
*Corresponding author email: munaltobi@gmail.com

Fawzi Yahya Wadday
Department of Chemistry, Faculty of Science, Kufa University, Al-Najaf-Iraq
Email: Fawzi.almuwashi@uokufa.edu.iq

Abstract---In this article, a synthesized ligand [5-amino 2-phenyl.4H-pyrazol-3-one] and it was used to prepare new complexes of Mn (II),Co(II), Ni(II), Cu(II), Zn(II), Pd(II) and Ag(I). The new ligand (HMABP) has categorized by Micro Elemental Analysis (C.H.N.S), UV-visible, Fourier Transform infrared (FTIR) approaches, ^{1}H,^{13}C-NMR spectroscopy and mass spectroscopy. The consequence has specified that the ligand was represented as N,N,O-tetradentate. The preparing of complexes has accomplished after fixing the finest concentration and pH. UV-Vis spectra of these complexes solutions have been examined for a range of pH (3-10) and concentration ($1x10^{-4}$-$5.5x10^{-4}$) Molar that comply with Lambert-Beers Law. A stoichiometry of the complexes has comprehended in relation to mole ratio which has gotten from spectroscopic investigations of the complex has solutions. The ratio of metal: ligand was achieved with (1:1) for all complexes. The metal ions complexes were characterized by FTIR, UV-Visible, molar conductance, atomic absorption, magnetic susceptibility, elemental analysis C.H.N.S techniques. From the results of physico-chemical and spectral techniques, octahedral geometry except with Pd^{2+} was square planar and tetrahedral shape with Ag^{+} have been proposed for these metal complexes. The TLC for (HMABP) ligand and its complexes have been depicted one spot for each one, signifying a completed formations of these compounds. All these compounds were evaluated against two kinds of human pathogenic bacteria gram positive and gram negative.

Keywords---spectral studies, complexes, azo, antibacterial activity, mass spectroscopy.

Introduction

The new chemical compound class azo-azomethane has been a topic of research over the past few years. The chemical properties of these compounds have been extensively studied in comparison to those of azo compounds and Schiff bases due to their two effective groups, the azo bridge (-N=N-) and azomethine (-N=C-) [(1)], these two groups contain a nitrogen atom with non-bonding pair electron, so it has electronic properties and selective structural flexibility toward metal ions. They act as stabilizing agents for metals in their low-valency oxidation states [(2)]. 5-amino-2-phenyl-4H-pyrazol-3-one is hetero electric defined with a 5-membered ring of 3 carbonates and 2 neighboring atoms of nitrogen are also considered as a weak base. Prominent medications which contain loop of pyrazole are silicoxib and activated steroids. New compounds of pyrazolone are of outstanding co-polymerization and undergo on rinse in organic solvents in the case of using them for eyes [(3)].

The coordination number[(5)], which is used in coordination chemistry to initially define a structure, is the sum of all the ligands that are linked to the metal, more specifically the sum of all the donor atoms. Even if the associated ligands can be counted, the counting method is yet unknown. Coordination numbers normally range from two to nine, despite the fact that extremely large numbers of ligands are common for lanthanides and actinides. The number of ligands, size, charge, and electron configuration of the metal ion, as well as the metal ions [(4)]. By developing a number of ligands that contained atoms capable of forming stable coordination bonds with metallic and other elements, researchers in the field of inorganic chemistry pioneered this field. Many academics and researchers are interested in coordination compounds because of their importance in a variety of fields, including the analytical side of metal extraction [(5)]. Azo compounds and Schiff bases are among the most significant organic ligands in the production of many coordination complexes by providing metallic elements with electrons[(6)]. The azo-azomethine ligands and their complexes were also used in the spectroscopy field because of their bright colors, used as antioxidants, inhibitors of corrosion [(7)], anticancer and antimicrobials[(8)]. As we have seen, Schiff base-azo and its derivatives are important molecules both in chemistry, biology and industrial biology and their complexes with metal ions are of particular interest in these fields.

Experimental Section

Instruments, materials and approaches

Entirely, the chemicals have bought from BDH and Fluka. Infrared Spectra of solid samples were recorded as (KBr) by a Shimadzu (FT-IR) spectrophotometer Ser.No.(604-8511), at Biochemical Central Laboratory Pharmacy college Kufa University. The range of measurement was (4000-400) cm^{-1}. The Uv-Vis Spectra of the compounds were obtained by using a Shimadzu in the range of (200-1100)nm, at Biochemical Central Laboratory Pharmacy college Kufa

University.The corrected melting points of prepared compounds have been measured in open capillary tubes by a Stuart melting point Engineering LTD.UK. Kufa University, College of Science. Elemental analysis of the ligands and some complexes were performed on a (C.H.N.S) at Sharif Sainte University, Tehran, Iran. ^{1}H and ^{13}C NMR spectra of (HMABP) ligand were recorded in DMSO-d6 at Sharif Sainte University, Tehran, Iran. Mass analysis of ligand and some complexes were performed at Tarbiat Modarres University, Iran. Metals content of the complexes were measured by using atomic absorption technique by Analytical Jena (A.A350) atomic absorption spectrophotometer in the laboratories of Ibn–Sina State Company, Hg metal is determined using Alhaydrid cold ablation system (HS 55) in Ibn Sina Company. Electrical conductivity measurements of the complexes were recorded at 25 °C for solutions of samples in DMSO solvent using using WTW inlab cond 720 digital conductivity meter. Biochemical Central Laboratory Pharmacy college Kufa University. Elemental microanalyses of the ligand and their complexes have implemented through Euro Vectro-3000A. The solutions and materials are employed in a biochemical analysis sterilized based on Autoclave, Gallen Kamp.

Synthesis of the ligand (HMABP)

The ligand was synthesized in two steps:

5-((2-hydroxy-4-methoxybenzylidene)amino)- 2-phenyl-2,4-dihydro-3H-pyrazol-3-one (Schiff base compound)

In general, the Schiff base compound was prepared by the reaction of the (1.521 g, 0.01 mol) 4-methoxysalicylaldehyde in 20 ml of absolute ethanol after adding 2-4 drops of glacial acetic acid with (1.751 g, 0.01 mol) 5-amino-2-phenyl-4H-pyrazol-3-one, the reaction mixture was refluxed for (3 hrs.), the progress of the reaction was followed by TLC using hexane–ethanol (3:7) (v/v) as eluent. After completion, the resulting mass was recrystallized from ethanol when a pale brown crystalline material was formed, melting point was found to be 115-117 ºC, and the yield was 81%. Rf (0.56). The scheme (1), represents the formation reaction of Schiff compound(9).

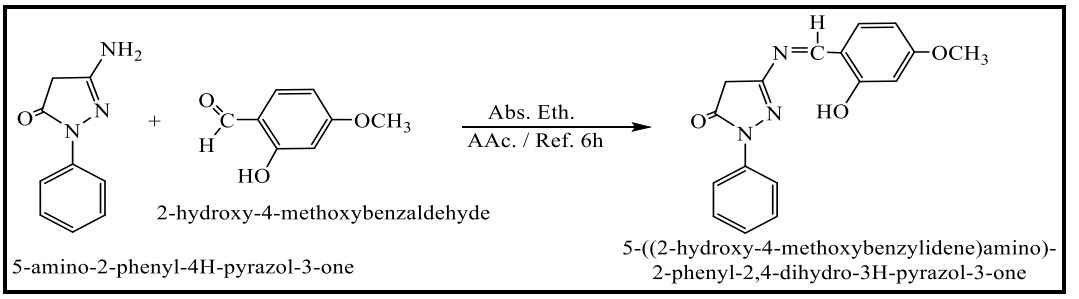

Scheme 1. Preparation reaction of Schiff base compound

Synthesis of 5-((2-hydroxy-4-methoxy-3-((5-methoxybenzo[d]thiazol-2-yl)azo)benzylidene)amino)-2-phenyl-2,4-dihydro-3H-pyrazol-3-one (HMABP)

The ligand was synthesized according to the general(10), method by dissolving (0.901 g, 0.005 mol) of 2-amino-6-methoxybenzothiazole in a mixture consisting of (3 mL) of con. hydrochloric acid ,(10mL) ethanol and (10 mL) of distilled water. The solution mixture was cooled under to (5 oC) then (0.69 g) (0.01 mol) sodium nitrite in (10 mL) distilled water solution was added dropwise with stirring in order to obtain the dizonium salt solution. After 20 min the dizonium solution was slowly added to a cooled basic ethanolic solution of (1.546 g, 0.005 mol) Schiff base compound a above in paragraph (2.1.3) and to obtain the (HMABP) ligand. The brown colored mixture was neutralized by dilute hydrochloric acid, sodium hydroxide and the solid precipitation was filtered off and washed several times with distilled water then left to dry at room temperature and recrystallized from with hot absolute ethanol, yield (83 %), Rf (0.51) and m.p oC (123-125), scheme (2), represents the formation reaction of ligand.

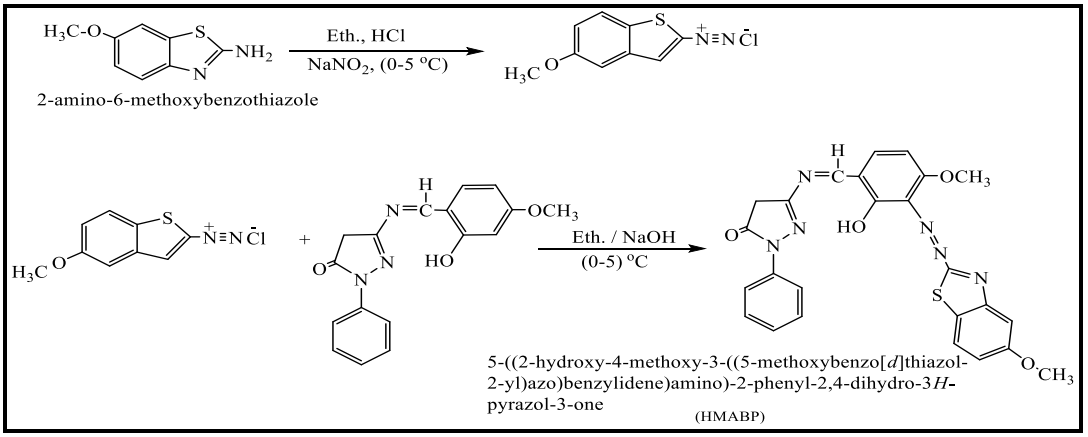

Scheme 2. Preparation reaction of ligand (HMABP)

Preparing the buffer solutions

Buffer solutions, covering the pH values from 3 to 10, of ammonium acetate (0.01mol) were prepared by dissolving (0.7708g) of CH_3COONH_4 in one liter of doubly distilled deionized water. The required pH was obtained by the addition of either ammonium hydroxide solution or glacial acetic acid.

Preparing the standard solutions

The ligand and metal salts standard solutions at a concentration of ($1x10^{-3}$ M) as stock solution was prepared by dissolving the required weight of ligand and metal salts (0.001 mol) in the (100) mL of ethanol. The solution was diluted similar to that of the metal salt solutions to obtain concentrations range ($1x10^{-4}$-$1x10^{-6}$ M).

Determination of optimum Concentrations

To determine the optimum concentrations for the mixing process, the solutions at ranged between ($1x10^{-3}$ - $1x10^{-6}$ M) for both the ligand and metal salts. Equal volumes were mixed for both the ligand and metal salts and measured the absorption value for these solutions. The high-ranged concentrations ($1x10^{-3}$ and $6x10^{-4}$ M) showed complexes precipitations for instant mixing of these solutions. So the concentrations between ($1x10^{-4}$-$5.5x10^{-4}$ M) were chosen because it gave acceptable absorption and some of them comply with the Per - Lambert law, as for the minimum concentration concentrations ($1x10^{-5}$ M and $1x10^{-6}$ M), they gave a weak measured.

Determination of optimum acid function

The effect of changing the acidic function at pH (3 - 10) to reach the optimum acidic function of the metal ions was studied after determining the optimum conditions, which included determining the optimum concentrations of ligand and metal ions.

Determination of standard calibration curve of the metal complexes

A solutions ranged between ($1x10^{-4}$-$5.5x10^{-4}$ M) for both the ligand and the metal salts studied, the equal volumes of same concentration of metal salts solutions and ligand solutions at optimum pH were mixed (one mL from each metal salt solution was mixed with one mL of ligand solution) at wavelength that gives the highest absorbance (λmax). The absorption values of these solutions in practical experiments showed that the optimal concentrations for complex prepared and suitable for spectral measurements fall within the range ($1x10^{-4}$-$5.5x10^{-4}$ M) were obeyed the Lambert-Pierre law

Synthesis of complexes

All chelation complexes were prepared by the same method and in (M:L) ratio (1:1), where (15 mL) ethanol solution of ligand (HMABP) (0.5g, 1mmol) was added slowly to (5 mL) buffer solution with an appropriate pH of (1 mmol of metal salt) in (10 mL ethanol) 0.197g $MnCl_2.4H_2O$, 0.238g $CoCl_2.6H_2O$, 0.237g $NiCl_2.6H_2O$, 0.170g $CuCl_2.2H_2O$, 0.136g $ZnCl_2$, 0.201g, 0.189g $AgNO_3$, 0.223g $Pd(CH_3CN)_2Cl_2$. A color change was observed after mixing both solutions and heating under reflux (1h) in ethanol to obtain complexes that were isolated in good precipitated yields. The precipitates were filtered off, washed with a mixture of (5:5) water : ethanol, dried, and then recrystallized from hot ethanol. Table (1), listed the quantity of ligand and yield percentage of all complexes and Scheme (3), shows the formation reaction of ligand complexes.

Table 1
Mass quantity, yield percentage and R_f for ligand and its complexes

Compound Formula	Wt.(g) of (1mmol)	Yield %	R_f
L=(HMABP) ($C_{25}H_{20}N_6O_4S$)	500.53	83	0.51

[Mn ($C_{25}H_{18}N_6O_4S$)Cl(H_2O)]	607.92	73	0.53
[Co ($C_{25}H_{19}N_6O_4S$)Cl(H_2O)]H_2O	629.93	77	0.55
[Ni ($C_{25}H_{19}N_6O_4S$)Cl(H_2O)]$2H_2O$	647.71	70	0.52
[Cu ($C_{25}H_{19}N_6O_4S$)Cl(H_2O)]H_2O	634.55	80	0.54
[Zn ($C_{25}H_{19}N_6O_4S$)Cl(H_2O)]$2H_2O$	654.40	68	0.55
[Ag ($C_{25}H_{19}N_6O_4S$)(H_2O)]H_2O	643.42	61	0.50
[Pd ($C_{25}H_{19}N_6O_4S$)Cl]	641.39	75	0.47

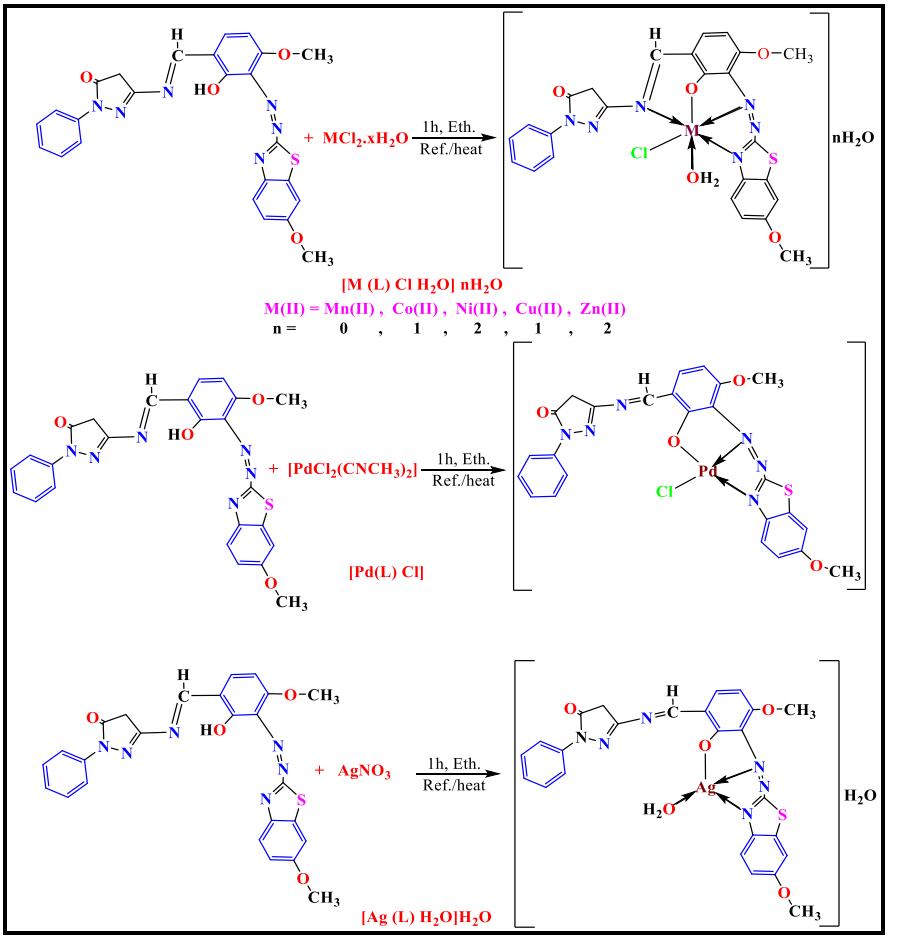

Scheme 3. Synthesis route of complexes

Consequences and Discussion

General

The ligand (HMABP) and its complexes are crystals, which are insoluble in water and soluble in common organic solvents. Many techniques have been used in

characterization of ligand and its metal complexes such as (FTIR, UV-Vis) spectra, magnetic susceptibility, mole ratio and molar electrical conductivity measurements. Also the elemental microanalysis (C.H.N.S), mass spectra used for characterization of some of complexes. The physical properties such as color, melting point and solubility, also have been dependent in characterization of metal complexes.

Physical Properties and Elemental Analyses

The physical properties and elemental microanalysis as well as metal content of complexes are described in Table (2). The (C.H.N.S) analysis and mass spectra have been done to all o complexes as examples of mononuclear complexes [11]. The atomic absorption technique helps us in determining the metal ion percentage at complex, so by which we can determine the (M : L) ratio in addition to mole ratio method. All of these results were in a good acceptance with the calculated values.

Table 2
Physical details and analytical information of ligand (HMABP) besides its complexes

Empirical formula	M.wt g. mol^{-1}	Color	M.P°C	Element analysis found (calc.)%				
				C	H	N	S	M
LH=(HMABP) ($C_{25}H_{20}N_6O_4S$)	500.533	Brown	123-125	th. 59.99 ex.(59.71)	4.03 (4.07)	16.79 (16.68)	6.41 (6.39)	-------
[Cr ($C_{25}H_{19}N_6O_4S$)Cl_2]	622.421	Nutty	197-199	48.24 (48.19)	3.08 (3.02)	13.50 (13.53)	5.15 (5.11)	8.35 (8.39)
[Mn ($C_{25}H_{19}N_6O_4S$)Cl(H_2O)]	607.928	purple	181-183	49.39 (49.42)	3.48 (3.53)	13.82 (13.78)	5.27 (5.29)	9.04 (9.08)
[Co ($C_{25}H_{19}N_6O_4S$)Cl(H_2O)]H_2O	629.938	Dark nutty	195-197	47.67 (47.41)	3.68 (3.71)	13.34 (13.37)	5.09 (5.06)	9.36 (9.39)
[Ni ($C_{25}H_{19}N_6O_4S$)Cl(H_2O)]H_2O	647.713	Dark purple	202-204	46.36 (46.49)	3.89 (3.95)	12.98 (12.93)	4.95 (4.97)	9.06 (9.12)
[Cu ($C_{25}H_{19}N_6O_4S$)Cl(H_2O)]H_2O	634.551	Dark Blue	212-214 D	47.32 (47.11)	3.65 (3.91)	13.24 (13.29)	5.05 (5.06)	10.01 (10.12)
[Zn ($C_{25}H_{19}N_6O_4S$)Cl(H_2O)]H_2O	654.400	Golden-Yellow	189-191	45.89 (45.81)	3.85 (3.73)	12.84 (12.89)	4.90 (4.93)	9.99 (9.95)
[Ag ($C_{25}H_{19}N_6O_4S$)(H_2O)]H_2O	643.423	Light red	184-186	46.67 (46.53)	3.60 (3.56)	13.06 (13.11)	4.98 (4.94)	16.76 (16.49)
[Pd ($C_{25}H_{19}N_6O_4S$) Cl]	641.395	Light Brown	247-249 D	46.82 (46.70)	2.99 (2.94)	13.10 (13.06)	5.00 (4.97)	16.59 (16.28)

Influence of pH

The influence of the pH of the complex solutions was also studied at pH range (3-10). To evaluated the optimum pH value from the illustrated in the Table (3) and Figures (1-7) which explained the relationship between pH value and the absorption values in ions solutions with the ligand (HMABP) used in this study, the determine pH depended on the fix absorption values at constant concentration for each solution.

Table 3
Absorbance at different pH and Optimum Concentration of (HMABP) metals ions solutions

pH	Abs at ($5x10^{-4}$) M						
	Mn(II) (480) nm	Co(II) (565) nm	Ni(II) (452) nm	Cu(II) (734) nm	Zn(II) (405) nm	Ag(I) (410) nm	Pd(II) (669) nm
3	0.046	0.021	0.017	0.038	0.027	0.011	0.071
4	0.05	0.032	0.019	0.042	0.031	0.013	0.075
5	0.056	0.041	0.02	0.044	0.038	0.014	0.084
6	0.06	0.056	0.022	0.052	0.043	0.016	0.092
7	0.074	0.08	0.027	0.0714	0.05	0.019	0.105
8	0.11	0.115	0.033	0.083	0.077	0.028	0.147
9	0.127	0.108	0.035	0.078	0.068	0.027	0.14
10	0.118	0.101	0.032	0.076	0.059	0.026	0.135

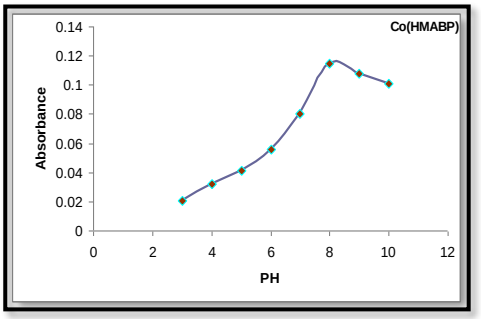

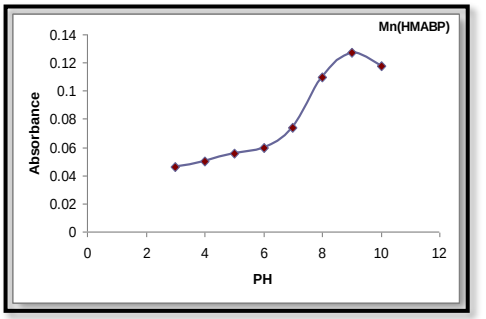

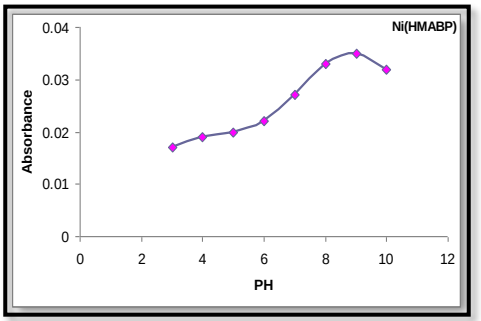

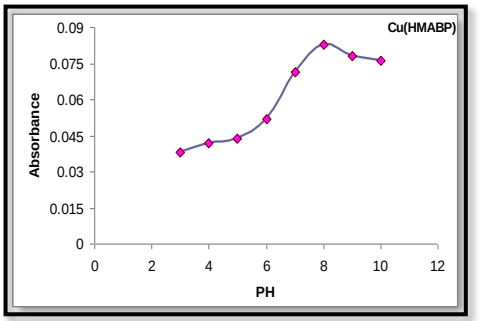

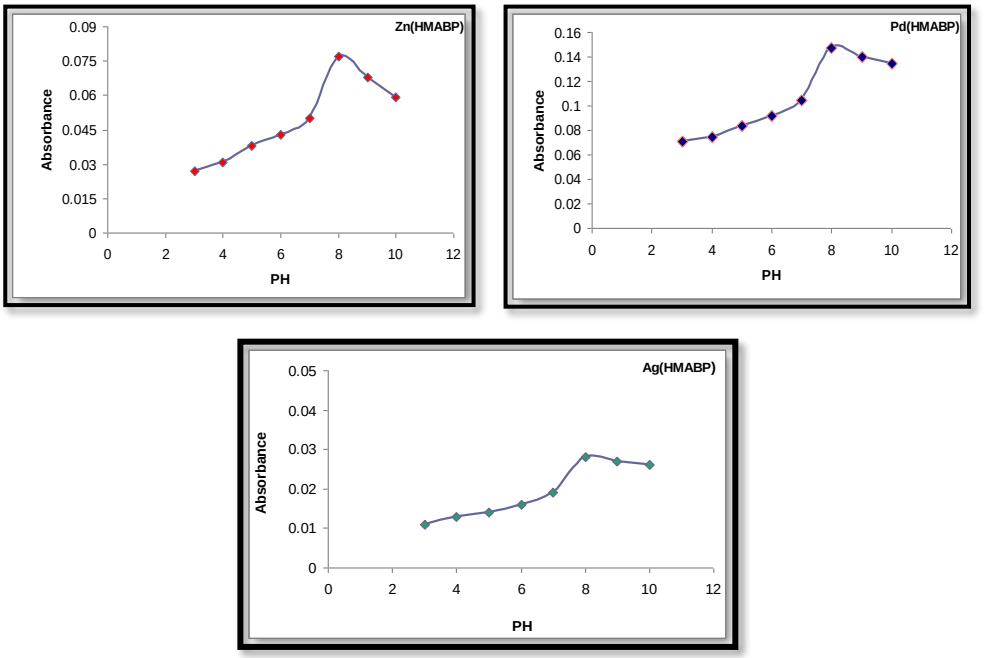

Figure 1-7. Effect of pH on absorbance at (λ_{max}) for the complexes at optimum concentration

There are many methods used to produce the best structure of complexes formed in solution without isolation [11]. The most familiar one is the mole ratio method. This method has been used frequently since its introduction by Yoe and Jones in (1944) [12]. The method is based on plotting measured absorbance against molar ratios of the two components of a complex when the concentration of one component is varied as the concentration of the other is held constant. If the system forms a stable complex that does not show appreciable dissociations such as a plot which gives a sharp break. . The measurements have been held at the concentration and wavelength. The results indicates the formation of (1:1) (metal : ligand) [12,13] ratio for all metal ions complexes.

NMR Spectra for the ligand (HMABP)

The ^{1}HNMR spectrum of (HMBP), Figure (8), in DMSO-d_6 showed protons signals due to the ligand symmetry. The single signal at (δ=10.00) ppm, 1H) assigned to (O-H) group [14], while the signal at (δ=9.02) ppm duo to (H-C=N) azomethine proton [15]. The aromatic proton were appeared at (δ=7.79-6.50) ppm and 8.57-7.20 ppm) due to benzene rings protons [16]. The signal at (δ=3.81 ppm) assigned to methyl proton (CH3-O) that attached with benzaldehyde ring whereas the (δ=3.46 ppm) assigned to methyl proton (CH3-O) that attached directly to the benzothiazole ring[21]. In addition to the singlet signal at (δ=2.06 ppm) assigned to methylene proton in pyrazoline ring[17]. The chemical shifts are illustrated in Table (4).

The ^{13}C-NMR spectrum of ligand (HMABP), Figure (9), in DMSO-d6 exhibited many chemical shifts, at δ(191.35 ppm) and (164.85 ppm) assigned to the atom (C4=O and C2=N) pyrazoline ring [18]. The chemical shifts appeared at δ(163.17 ppm) and (154.35 ppm) assigned to the (C32=N) and (C21=N) carbon atoms of benzothiazole ring and azomethine respectively [19]. The chemical shift at δ(146.82 ppm) assign to (C8, C15, C27) in benzene and benzothiazole aromatic rings carbon atoms (20) and the chemical shift appeared at δ(132.29 ppm) duo to (C10,C11,C12) carbons, while the shift at δ(131.97 ppm) attributed to (C9 , C13 , C29), whereas the shift at (128.78 ppm) assigned to (C14 , C24) atoms and the chemical shift appeared at (123.02 ppm) duo to (C13 , C16) carbon atoms, while the shift at (118.13 ppm) was assigned to (C26). The chemical shifts appeared at δ(112.91, 105.57) and (107.49) ppm were assigned to (C17, C19 and C25) benzene and benzothiazole rings carbons while the shift at (100.81 ppm(duo to (C18) aromatic carbon atom, these chemical shits mentioned previously from (C8 to last atom C18) attributed to carbon atoms of benzene and benzothiazole aromatic rings [20,21]. The shifts at (55.70-55.56 ppm) duo to (C36 , C37) methoxy groups carbon atoms [22] shifts appeared at δ(37.35 ppm) was assigned to the carbon atoms of (C3) in pyrazoline ring [23]. The chemical shifts are shown in Table (5).

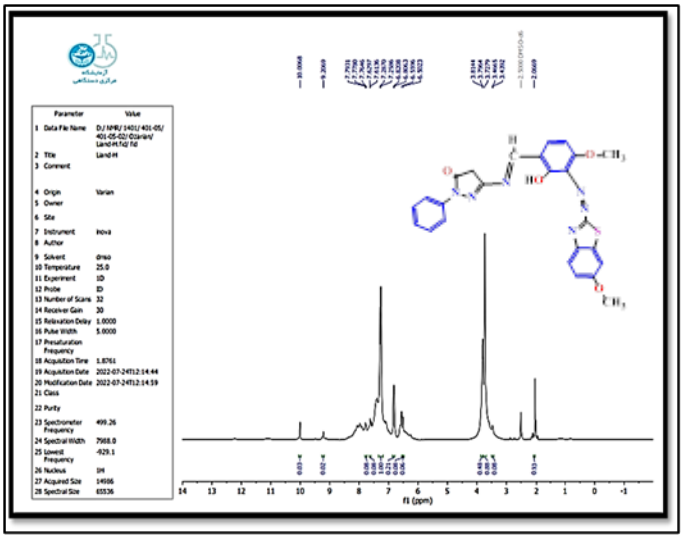

Figure 8. ^{1}H-NMR spectrum of the ligand (HMABP)

Table 4
^{1}H-NMR spectral data, chemical shifts and assignments of ligand (HMABP) in DMSO-d_6

Compound symbol	Chemical shifts δ(ppm) (no. of protons)	Assignment
(HMABP)	(10.00) (1Hs)	(O-H) proton
	(9.20) (1Hs)	(H-C=N) azomethine proton
	(7-79 - 6.50) (10H)	Aromatic rings protons

	(3.81) (3Hs)	(CH_3-O)-benzaldehyde
	(3.46) (3Hs)	(CH_3-O)-benzothiazole
	(2.06) (2Hs)	(C-H) methylene pyrazoline

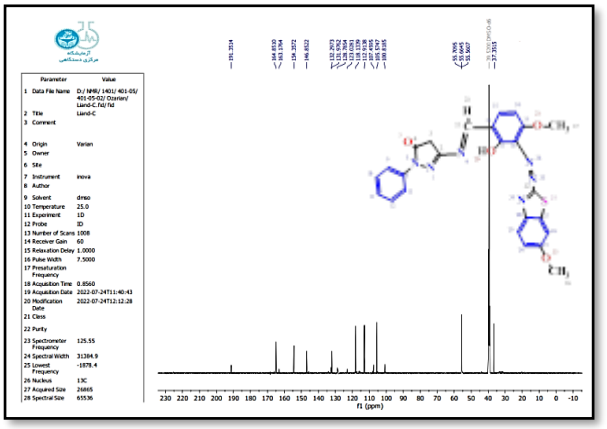

Figure 9. ^{13}C-NMR spectrum of ligand (HMABP)

Table 5
^{13}C-NMR spectral data and chemical shifts assignment of ligand (HMABP)

Compound symbol	Chemical shifts δ(ppm)	Assignment
(HMABP)	(191.35) and (164.85) (163.17) (154.35) (146.82) (132.29) (131.97) (128.78) (123.02) (118.13) (112.91 and 107.49) (100.81) (55.70 - 55.56) (37.35)	(C_2=O and C_4=N) pyrazoline ring (C_{32}=N) benzothiazole ring (C_{21}=N) azomethine (C_8, C_{15}, C_{27}) (C_{10},C_{11}, C_{12}) (C_9 , C_{13} , C_{29}) (C_{14} , C_{24}) (C_{13} , C_{16}) benzene and benzothiazole (C_{26}) (C_{17}, C_{19} and C_{25}) (C_{18}) (C_{36} , C_{37}) (C_3) pyridine rings

Mass spectrum for the azo ligand (HMABP)

Many previously reported studies[24] depending on proposing the fragmentation pathways of prepared ligand.. Mass spectrum of (HMABP), Figure (10), showed the mother ion peak at (m/z+=501.4), as parent ion peak which related to (M++H), this is consider good evidence to prepared the new ligand. The others fragment and their relative abundances and fragmentation pathways are shown in Table (5) and Scheme (4).

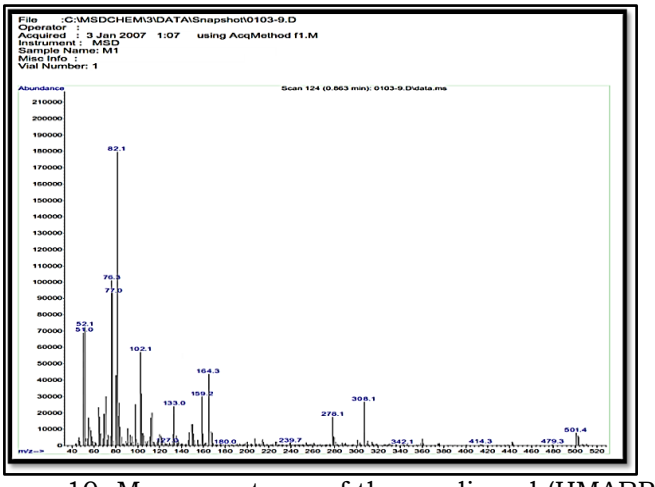

Figure 10. Mass spectrum of the azo ligand (HMABP)

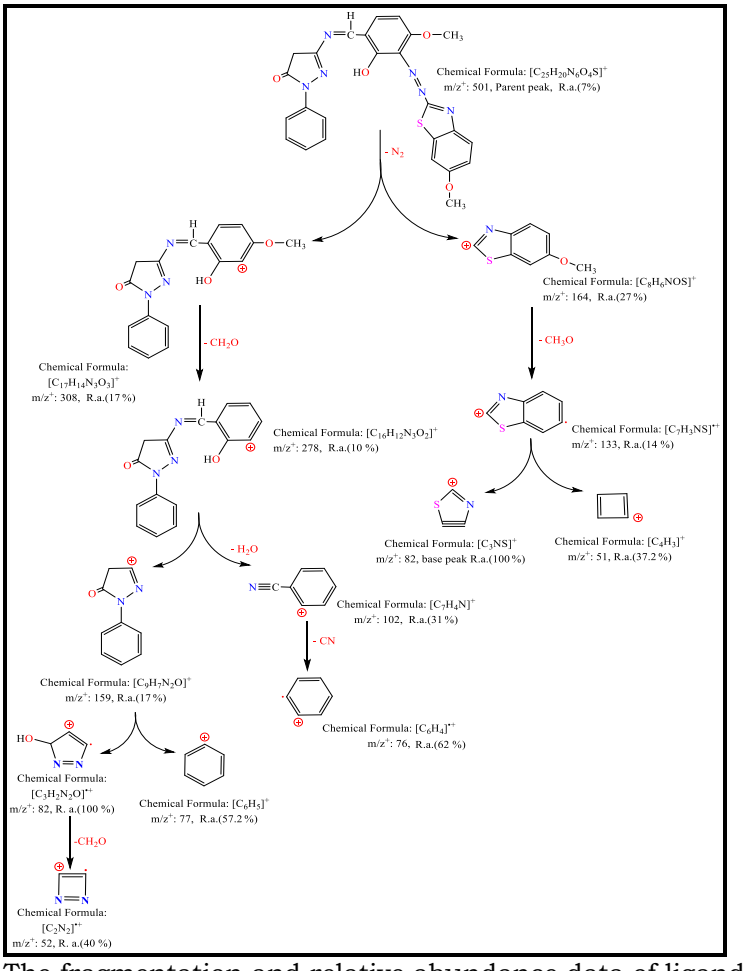

Scheme 4. The fragmentation and relative abundance data of ligand (HMABP)

UV-Vis Spectral studies

The (UV-Vis.) spectrum of ligand, Figure (11), in ethanol exhibited first high intensity absorption peak at (241 nm), (270 nm) and (320 nm) assigned to (π→π*) transitions. The absorption band at (400 nm) which attributed to (n→π*) transitions a result from presence of lone pairs of electrons [25]. The data illustrated in Table(6). The electronic spectra of the metal complexes solution in ethanol showed the bands corresponding to the intraligand $\pi\rightarrow\pi^*$and $n\rightarrow\pi^*$ transitions shifted to lower energy, this observation in the metal complexes is relative to the free ligand have been attributed to complexation.

The electronic spectrum of manganese ion complex showed two weak absorption bands, the first band at (480 nm) is due to the ML-C.T. The second absorption band at (650 nm) is assigned to $^6A_1g_{(G)}\rightarrow{}^4T_1g_{(G)}$, transitions in octahedral (^6S) [26]. Cobalt ion complex gives dark nutty color and its electronic spectrum Figure (12), exhibited two bands appeared at (565 nm) and (679 nm) which were assigned to the $^4T_1g_{(F)}\rightarrow{}^4T_1g_{(p)}$ (υ_3) and $^4T_1g_{(F)}\rightarrow{}^4A_2g_{(F)}$ (υ_2) transitions respectively of octahedral geometry [27]. Nickel complex Figure (3-32), showed three bands in the visible region at (452 nm) $^3A_2g(F)\rightarrow{}^3T_1g_{(F)}$ (υ_3), (724 nm) $^3A_2g_{(F)}\rightarrow{}^3T_1g_{(F)}$ (υ_2) and the last one is at (959 nm) $^3A_2g_{(F)}\rightarrow{}^3T_2g_{(F)}$, ($\upsilon_1$) [28]. Copper (II) complex Figure (3-33), showed broad band at (734 nm) assigned to $^2Eg\rightarrow{}^2T_2g$ transition which refers to Jahn-Teller distortion of octahedral geometry [29]. Pd(II) spectrum displayed high intensity peak at (669 nm) was attributed to ($^1A_1g\rightarrow{}^1B_1g$), whereas the new at (573 nm) were attributed to electronic transition type $^1A_1g\rightarrow{}^1A_2g$ [30]. Electronic transition spectra of Zn(II) and Ag(I) complexes gaves only one band with tail in lower energy for each complex compared with ($\pi\rightarrow\pi^*$) and ($n\rightarrow\pi^*$) transitions for the free ligand transition these attributed to intra-ligand charge transfer (M→L,C.T) transition (405 nm) at Zn(II) and (410 nm) with Ag(I) complexes are observed respectively [31], with change in its shape, intensity and position compared with free ligand.

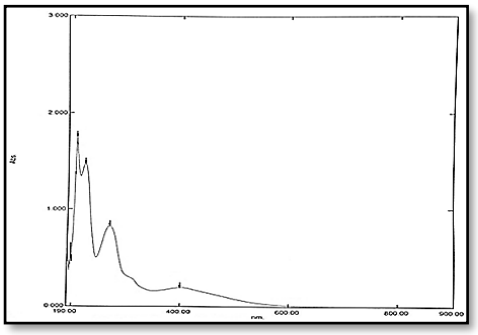

Figure 11. UV-Vis spectrum of (HMABP)

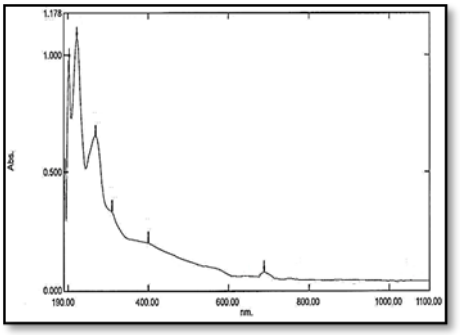

Figure 12. UV-Vis spectrum of (Co) complex

Table 6
Electronic spectra of ligand (HMABP) and it's metal ions complexes in ethanol

Complex	Band position nm	Band position cm^{-1}	Assignments	Geometry	Hybridization
Ligand (HMABP)	241 270 320 400	41493.77 37037.03 31250 25000	$\pi\rightarrow\pi^*$ $\pi\rightarrow\pi^*$ $\pi\rightarrow\pi^*$ $n\rightarrow\pi^*$	-------	------
L-Mn(II)	480 650	20833.33 15384.61	M→L,C.T $^6A_1g_{(G)}\rightarrow{}^4T_1g_{(G)}$	Octahedral	SP^3d^2 (high spin)
L-Co(II)	565 679	17699.11 14727.54	$^4T_1g_{(F)}\rightarrow{}^4T_1g_{(p)}$ $^4T_1g_{(F)}\rightarrow{}^4A_2g_{(F)}$	Octahedral Distorted	SP^3d^2 (high spin)
L-Ni(II)	452 724 959	22123.89 13812.15 10427.52	$^3A_2g\rightarrow{}^3T_1g_{(p)}$ $^3A_2g\rightarrow{}^3T_1g_{(F)}$ $^3A_2g\rightarrow{}^3T_2g_{(F)}$	Octahedral	SP^3d^2 (high spin)
L-Cu(II)	734	13623.97	$^2Eg\rightarrow{}^2T_2g$	Octahedral Distorted	SP^3d^2
L-Zn(II)	405	24691.35	M→L,C.T	Octahedral	SP^3d^2
L-Ag(I)	410	24390.24	M→L,CT	Tetrahedral	SP^3
L-Pd(II)	398 669 573	25125.62 14947.68 17452..06	n→π*(-N=N-), (-C=N) C.T ($^1A_1g\rightarrow{}^1B_1g$) ($^1A_1g\rightarrow{}^1A_2g$)	Square planar	dSP^2

IR Spectra of Ligands and Complexes

The FTIR spectra of (HMABP) and its complexes showed disappearance a broad band at (3395) cm^{-1} assigned to ν(O-H) vibration hydroxyl group in the free ligand [31], but a new broad band at high energy than in the ligand carboxyl group appeared in some of the complexes spectra such as (3401 with Mn^{2+}, 3405 with Co^{2+}, 3404 with Ni^{2+}, 3409 with Cu^{2+}, 3410 with Zn^{2+} and 3414 cm^{-1} with Ag^{+}) these due to the coordination of the water as a ligand in coordination sphere [32]. In all the complexes, bands which appeared at (1683) cm^{-1} in L-Mn, band at

(1678) cm^{-1} in L-Co, band at (1686) cm^{-1} L-Ni, band at (1672) cm^{-1} to L-Cu, band at (1679) cm^{-1} in L-Zn, band at (1683) cm^{-1} in L-Ag and band at (1679) cm^{-1} in L-Pd complexes are due to stretching vibration of the pyrazoline carbonyl group in these complexes spectra, this band stretching was a very slight frequencies change in these complexes when it's compared with that band shape and energy in the free ligand spectrum, that means no involvement of (C=O) group in coordination [33].

The FTIR spectrum of free ligand (HMABP) exhibited a strong bands at (1600) cm^{-1} and at (1575) cm^{-1}which were assigned to υ(C=N) groups vibrations of azomethine and benzothiazole ring respectively [34], these bands were shifted to lower frequencies with noticeable change in their shape in the spectra of all the complexes [35]. These differences are considered a good indicator for coordination of the metal ions with nitrogen atom of azomethine and benzothiazole ring. The υ(N=N) stretching vibration exhibited band at (1498) cm^{-1} in the free ligand spectrum shifted to lower frequencies at range (1479-1471) cm^{-1} with difference in its shape and intensity in spectra of prepared complexes [37], this shift of frequency given us clear evidence about the coordination of metal ion with (N) atom of azo group and delocalization of electron density between metal ion and ligand (π-system) [35,36]. A new bands showed in the complexes spectra which were not present in spectrum of the free ligand, this bands were located at range (514-498) cm^{-1}which was assigned to ν(M-N), while other new bands were observed at (498-430cm^{-1}) refers to ν(M-O) [37]. These observations in spectra of free ligand and its complexes indicated that the metal ions coordinate with ligand via (N, O, N,N) of pyrazoline ring, azo, azomethine and (O) atoms of hydroxyl group that attached benzene ring, behaving tridentate ligand toward metal ions. The disappearance of υ(M-Cl) vibration band in the complexes spectra that containing coordinated is attributed to the energy of this band is outside the measurement range of the device. Figures (13-14), Further details of characteristic bands and assignments are listed in Table (7).

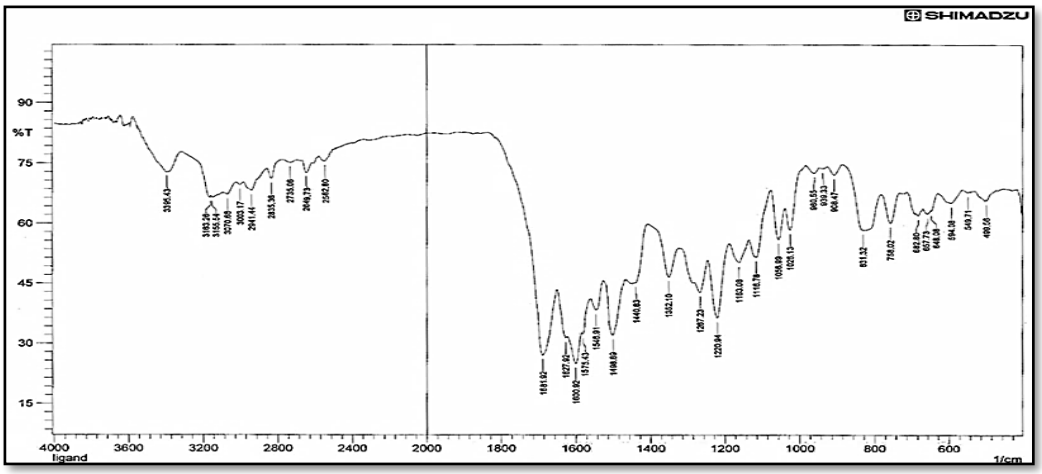

Figure 13. FT-IR spectrum of ligand (HMABP)

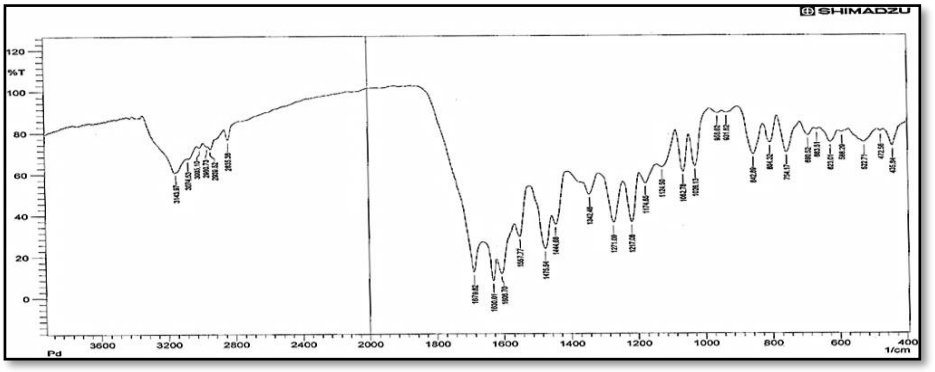

Figure 14. FTIR spectrum of (Pd) complex

Table 7
FTIR spectral data (cm^{-1}) of (HMABP) and it's metal complexes

Compound	υO-H + Coord.Hydrate	υC=O pyrazoline	υC=N pyrazoline	υC=N azomethine	υC=N benzothiazole	υN=N Azo	δH_2O aqua	υM-N	υM-O
L=(HMABP)	3395	1681	1627	1600	1575	1498	-	-	-
L-Mn	3401	1683	1631	1583	1558	1475	871	473	435
L-Co	3405	1678	1633	1581	1556	1477	860	472	437
L-Ni	3404	1686	1630	1583	1558	1475	862	475	433
L-Cu	3409	1681	1628	1578	1556	1476	865	476	441
L-Zn	3410	1679	1632	1578	1557	1478	879	487	437
L-Ag	3414	1683	1627	1600	1558	1472	875	468	433
L-Pd	-	1679	1630	1606	1556	1475	-	472	435

Magnetic Moment and Molar Conductance of Prepared Metal complexes

The calculated magnetic values at some complexes well agree with the taken values from spin moments of a high spin octahedral geometry, but low spin with the other complexes such as tetrahedral shape with silver and square planar shape with palladium and platinum complexes [38]. The molar conductance values of all complexes in DMSO as solvent at ($1x10^{-3}$ M) concentration were in the range (7.88 - 11.21 $S.cm^2.mole^{-1}$) indicating the (0:0) ratio electrolyte nature, this means that all the prepared complexes were non-electrolytes [39]. The molar conductivity values and magnetic values of all prepared complexes are listed in Table (8).

Table 8
Molar conductance values in DMSO and Magnetic moment of complexes

Complexes formula	μ_{eff}(B.M)	Λ_M ($S.cm^2.mol^{-1}$)
(HMABP)-Mn	5.91	9.61

(HMABP)-Co	4.74	7.9
(HMABP)-Ni	3.08	11.21
(HMABP)-Cu	1.79	7.88
(HMABP)-Zn	Dia.	10.06
(HMABP)-Ag	Dia.	8.06
(HMABP)-Pd	Dia.	10.21

Antimicrobial activity

Ligands and their complexes are of great importance in the biological field in the inhibition of biological activity [40] because many types of pathogenic bacteria to contain these compounds, hybrid atoms such as oxygen, nitrogen and sulfur are qualified to bond with different elements so we decided to study the biological activity of the new link (HMABP) And its complexes prepared with the studied metal ions of two types of pathogenic bacteria (*Staphylococcus aureus*-Gram-positive and *Escherichia coli*-Gram Negative) on which agar (Muller Hinton) grows at a temperature of 37 °C [41]. The results of all tested compounds showed the ability to inhibit the growth of bacteria used in two types of Gram-positive and negative stains. Regarding the selected bacterial response, we observed the significant biological effect of the ligand and its complexes studied at the previous concentration with pathogenic bacteria (*Sta. aureus*) [42] . Either with *E. coli*, which is a Gram-negative bacterium, and it showed somewhat less response to the ligand and its complexes studied than the other type of bacteria, and it was characterized by its resistance to many chemical compounds and antibiotics [43]. The reason for this resistance is the colon bacteria that are found in a single bacillus that contains a thick envelope surrounding its cell, and this coating contains a high percentage of lipids that resist these substances from entering the cell, while Sta. aureus bacteria do not have this property, so they will be less resistant to the penetration of chemicals and antibiotics into the bacterial cell [44]. The inhibition regions of the new ligand and its compounds (mm) were scored for their antibacterial activity against both types of pathogenic bacteria. It is shown in Table(9).

Table 9
The data of antibacterial activity (zone of inhibition) (mm) of ligand (HMABP) and its complexes at ($1x10^{-3}$M)

Compound	Pathogenic bacteria	
	Sta. aureus - Gram(+)	*E. coli* - Gram(-)
Control (S) DMSO	6	6
Ligand	16	13
L-Mn	18	17
L-Co	18	16
L-Ni	19	18
L-Cu	19	17
L-Zn	20	18
L-Ag	20	19

L-Pd	19	18

Conclusion

The present work describes the synthesis of a series of transition metal complexes have been synthesized from the new Schiff base-azo ligand (HMABP) derived from (5-amino-2-phenyl-4H-pyrazol-3-one) as starting materials. The ligand which was prepared and its metal complexes where characterized by physic-chemical spectroscopic techniques such as: FT-IR, UV-Vis spectra, (C.H.N.S) data, molar conductivity, magnetic moment, mass spectrometry, NMR and microanalysis techniques. As part of program directed toward the transformation of (HMABP) into metal complexes. The synthesis of (Mn^{2+}, Co^{2+}, Ni^{2+}, Cu^{2+}, Zn^{2+}, Ag^{+}, Pd^{2+}) metal complexes resulted in the formation of complexes with molar ratio (1:1) (M:L). On the basis of FT-IR, UV-Vis. spectra, elemental analysis, atomic absorption, molar conductivity, and magnetic susceptibility studies for the metal ions complexes, as well as ^{1}H, $^{13}CNMR$, Mass measurements for some of complexes. The new (HMABP) ligand acted as a tetradentate type (N, O, N, N) donor with Mn, Co, Cu, and Zn metals ions through the nitrogen atom of azomethine group, oxygen atom of hydroxyl methylacetophenone, nitrogen azo group, and nitrogen of methoxybenzothiazole and its tridentate type (O, N, N) donor with Pd, and Ag ions. In addition to chloride ion and one water molecule as aqua contributed to the coordination sphere in octahedral geometry, but tetrahedral complex with Ag+ and square planar complex with Pd^{2+}. All these compounds were evaluated against two kinds of human pathogenic bacteria gram positive and gram negative.

Acknowledgment

I would like to express my sincere gratitude to the faculty members of the Department of Chemistry, College of Science. My thanks and gratitude to Dr. Fawzi Yahya Wedday for his research support during the work period.

References

1. Abd Alamee, J. S., and Kareem, I. K. NeuroQuantology, 20 (1), (2022): 62-70.
2. Adnan, Sh., Egyptian Journal of Chemistry, 63 (12), (2020): 4749-4756.
3. Al-Adilee, J., and Jaber, A., Asian Journal of Chemistry, 30(7) (2018): 0000-0000.
4. Ali, A. E., Shokry, A. A,, and Kolkaila, S. A. Journal of Chemical Research Advances, , 2 (2), (2021): 1-9.
5. Antil, N., Kumar, M., Verma, K. K., & Garg, S., Asian Journal of Chemistry, (5), (2022): 1125-1133
6. Arunadevi, A., Porkodi, J., Ramgeetha, L., & Raman, N. , Nucleotides and Nucleic Acids, 38(9), (2019): 656-679.
7. Azam, M., Al-Resayes, S. I., Wabaidur, S. M., Altaf, M., Chaurasia, B., Alam, M. and Park, S., Molecules 23 (4), (2018): 813.
8. Clementina, M., Santos, M., Vera, L., Silva, M., andArtur M. S., Silva Molecules, 22 (10),(2017):1- 47.
9. Demehin ,A.I., Oladipo ,M. A. and Semire, B., The Egyptian Journal of Chemistry, (62), (2019): 413 - 426.

10. Deswal, Y., Asija, S., Dubey, A., Deswal, L., Kumar, D., Jindal, D. K., & Devi, J., antidiabetic and molecular docking, (2022).
11. Devi, J., Sharma, S., Kumar, S., Kumar, B., Kumar, D., Jindal, D. K., & Das, S. Applied Organometallic Chemistry, 36(8), (2022): e6760.
12. El-Boraey, H. A., AboYehia ,S., M., and El-Gammal ,O. A. Applied Radiation and Isotopes, 182, (2022): 110121.
13. Hameed, G. F., Wadday, F. Y., Farhan, M. A. A. and Hussain, S. A., Egyptian Journal of Chemistry, 64 (3), (2021): 1333 - 1345.
14. Hassan, A. M., Heakal, B. H., Soliman, O., Abdalla, K., & Abo El-ata, W. , Egyptian Journal of Chemistry, 62 (3), (2019): 401-414.
15. Ibraheem I. H., Mubder, N. S., Abdullah, M. M., Al-Neshm, H.,Baghdad Science Journal, 19(4), (2022) :114-120.
16. Kasare, M. S., Dhavan, P. P. Jadhav, B. L. and Pawar ,S. D. ChemistrySelect, 4 (36), (2019):10792-10797.
17. Kastas ,G., Albayrak Kastas, C., Ersanlr, C. C. , and Kosar Kirca, B. Crystallography Reports, 65(3), (2020): 463-467.
18. Koval'chukovaa ,O. V., Strashnovaa, O. V. Avramenkoa, M. A. Ryabova , C. Anitha, C. D. Sheela, P. Tharmaraj,3 and V. V. Hema - Journal of Chemistry Volume, (2013): Article ID 724163, 12 pages http://dx.doi.org/10.1155/2013/724163
19. Krishnaswamy, D., Govande, V.V., Gumaste, V. and Bhawal, B.M., Tetrahedron, 58(11), (2002): 2215–2225 methylphenol Copper (II) Complex"", 2014
20. Lawrence, G.A. Introduction to coordination chemistry, 2nd. Ed., John Wiley and Sons Ltd., United Kingdom, (2010).
21. Lekaa, K. A.and Saba, H. M.; The 1st International Scientific Conference On Pure Science, 1234, (2019): 1-13.
22. Mahdi, S. H. , Abdul Karem, L. K., International Journal of Pharmaceutical Research , (1), 2020: 1734-1740
23. Mahmudov, K. T., Gurbanov, A. V., Aliyeva, V. A., Resnati, G., & Pombeiro, A. J. Coordination Chemistry Reviews, 418, (2020): 213381.
24. Masoud, M. S. , Ali ,A, E., Abd Elfatah, A. S., Amer, G. E., Open Journal of Inorganic Non-metallic Materials, 11(1), (2021): 1 -22.
25. Merdas, S. M ., Annals of R.S.C.B., ISSN, 25 (4), (2021): 910-928.
26. Mishra, N., et al. Results in Chemistry, 1, (2019): 100006.
27. Ndifon, P., Kuate, M., Ngandung, E., Paboudam, A. G., Mariam, C. A., Peucheu, C., and Tonle, K. I., Egyptian Journal of Chemistry, 65(9), (2022): 477-495.
28. Ndifon, P., Kuate, M., Ngandung, E., Paboudam, A. G., Mariam, C. A., Peucheu, C., and Tonle, K. I., Egyptian Journal of Chemistry, 65(9), (2022): 477-495.
29. Pan, H., Ganose, A. M., Horton, M., Aykol, M., Persson, K. A., Zimmermann, N. E., & Jain, A.. Inorganic chemistry, 60(3),(2021): 1590-1603.
30. Patil, V. S., Dhanshri V. P., and Sachin S. P.. Commun., 15(1), (2022) :71-80.
31. Pereira, G. A., et al. Polyhedron, 38(1), (2012): 291-296.
32. Prasad, A. S., and. Rao, K. V. Applied Microbiology and Biotechnology, 97 (16), (2013): 7469-7481.
33. Qi, J., Luo, Y., Zhou, Q., Su, G., Zhang, X., Nie, X., ... & Li, W. Journal of Molecular Structure, 1255, (2022): 132458.

34. Radwan, I.T, Elwahy, A. H, Darweesh, A. F., Sharaky, M., Bagato, N., Khater, H. F., Salem, M. E., Journal of Molecular Structure, (2022): 6:133454
35. Richert, M., et al. Dalton Transactions,48(28), (2019): 10689-10702.
36. Saba, H.M. , Al-Azzawi; A .,Thesis, University of Baghdad Department of Collage of Education Ibn Al-Haitham,(2018).
37. Samia, M. M, ISSN:1583-6258, 25(4), (2021) : 910 – 928.
38. Sarkar, S., Banerjee, A., Halder, U., Biswas, R., and Bandopadhyay, R. Water Conservation Science and Engineering 2(4), (2017): 121-131.
39. Shibata, S., Furukawa, M. and Nakashima, R., Anal. Chim. Acta, 81, (1976): 131-141.
40. Siraj, I. T., and S. Sanusi. International Journal of Scientific Research in Chemistry (IJSRCH), 6 (4), (2021): 01-09.
41. Siraj, I. T., and S. Sanusi. International Journal of Scientific Research in Chemistry (IJSRCH), 6(4), (2021): 01-09.
42. Toole, N., Lecourt, C., Suffren, Y., Hauser A., Khrouz, L. and Desroches, C., European J. of inorganic chemistry, (1), (2019): 73-78.
43. Von der Stück, R., Krause, M., Brünink, D., Buss, S., Doltsinis, N. L., Strassert, C. A., & Klein, A. Zeitschrift für anorganische und allgemeine Chemie, 648(1), (2022): e202100278.
44. Wadday ,F. Y., Ahmed Ali Hussein, Research Journal of Pharmacy and Technology , 5(8), (2022):DOI: 10.52711/0974-360X.2022.00578
45. Yadav, M., Sharma, S., and Jai D. Journal of Chemical Sciences 133(1), (2021): 1-22.
46. Yoe, J. H., and A., Jones Letcher Industrial & Engineering Chemistry Analytical Edition, 16(2), (1944): 111-115.